Enzymatic sensor for phenols based on titanium dioxide generating surface confined ROS after treatment with H_2O_2

Enzymatic sensor for phenols based on titanium dioxide generating surface confined ROS after treatment with H_2O_2

Vanoushe Rahemi[a,b], Stanislav Trashin[a], Zainab Hafideddine[c], Vera Meynen[b], Sabine Van Doorslaer[c] and Karolien De Wael[a,*]

[a]*AXES research group, Department of Chemistry, University of Antwerp, Groenenborgerlaan 171, 2020 Antwerp, Belgium*

[b]*Laboratory of Adsorption and Catalysis (LADCA), Department of Chemistry, University of Antwerp, Universiteitsplein 1, B-2610 Wilrijk, Belgium*

[c]*Department of Physics, University of Antwerp, Universiteitsplein 1, B-2610 Wilrijk, Belgium*

[*]*Corresponding author. E-mail address: karolien.dewael@uantwerpen.be*

Highlights

- Short treatment by H_2O_2 activates TiO_2 to support peroxidase-based catalysis
- EPR reveals the presence of ROS at TiO_2 surface after treatment with H_2O_2
- A more sensitive approach is designed for the detection of phenolic pollutants

Graphical abstract

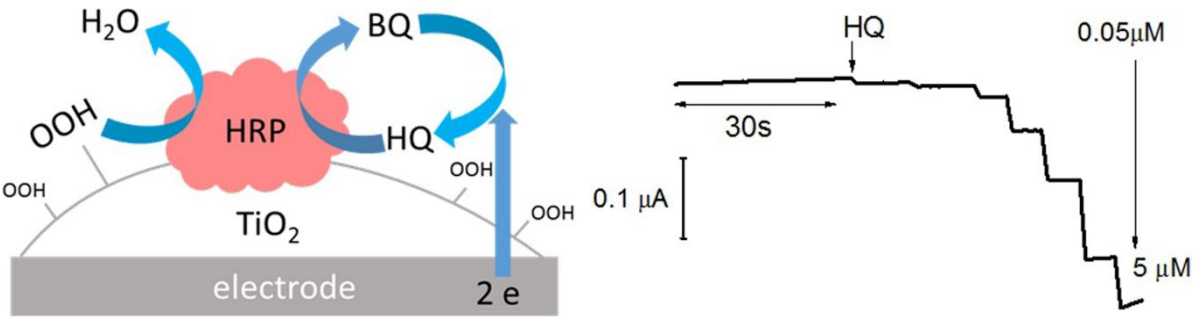

Abstract

Titanium dioxide (TiO_2) is a popular material as host matrix for enzymes. We now evidence that TiO_2 can accumulate and retain reactive oxygen species after treatment by hydrogen peroxide (H_2O_2) and support redox cycling of a phenolic analyte between horseradish peroxidase (HRP) and an electrode. The proposed detection scheme is identical to that of second generation biosensors, but the measuring solution requires no dissolved H_2O_2. This significantly simplifies the analysis and overcomes issues related to H_2O_2 being present (or generated) in the solution. The modified electrodes showed rapid stabilization of the baseline, a low noise level, fast realization of a steady-state current response, and, in addition, improved sensitivity and limit of detection compared to the conventional approach, i.e. in the presence of H_2O_2 in the measuring solution. Hydroquinone, 4-aminophenol, and other phenolic compounds were successfully detected at sub-μM concentrations. Particularly, a linear response in the concentration range between 0.025 and 2 μM and LOD of 24 nM was demonstrated for 4-aminophenol. The proposed sensor design goes beyond the traditional concept with three sensors' generations offering a new possibility for the development of enzymatic sensors based on peroxidases and the formation of ROS on titania after treatment with H_2O_2.

Keywords: Horseradish peroxidase; Titanium dioxide; Hydrogen peroxide; Hydroperoxyl species; Bioelectrochemistry

1. Introduction

Given the importance of water to all life forms, the presence of pollutants in water has garnered considerable attention. Recent methodologies in contaminants identification have designated phenols as priority pollutants [1, 2] and international regulatory organizations have set strict discharge limits for phenols [3]. Therefore, there is an urge for robust, easy-to-operate, and low-cost sensors to monitor and detect phenolic contaminants.

Numerous enzymatic biosensors have been suggested to detect phenolic compounds [4-8]. Among others, peroxidases, *e.g.* horseradish peroxidase (HRP), are favourable enzymes in such sensors due to a high catalytic activity towards a wide range of phenolic substrates [8-13]. However, HRP requires hydrogen peroxide (H_2O_2) as a co-substrate that plays the role of a sacrificial electron acceptor in the sensing mechanism for phenols. The addition of H_2O_2 complicates the analysis and increases the background noise because H_2O_2 is essentially electroactive and it contributes to the background current [14]. Therefore, the catalytic oxidation of phenolic compounds with a HRP-based biosensor in the presence of H_2O_2 is challenging. Thus, it is of significant interest to develop a hydrogen peroxide-less HRP based biosensor for the detection of phenolic compounds.

A few ideas were developed to avoid adding H_2O_2 during analysis by HRP-base biosensors. Munteanu et al. [15] suggested generation of H_2O_2 in flow by glucose oxidase in the presence of oxygen and glucose which are long-term stable. This offers a more gentle way to introduce H_2O_2 but cannot solve the issue of an increased background current and noise. Other works explored usage of phenol oxidases (mostly laccase and tyrosinase) as alternative biocatalysts and focused the efforts on improving the sensor sensitivity by adding conductive nanomaterials and optimizing the enzyme immobilization on the composite layers [16-18]. An interesting strategy was describe by Chang et al [19], who prepared a tyrosinase-peroxidase bi-enzyme sensor that does not require the exogenous addition of H_2O_2 due to simultaneous generation of H_2O_2 at the electrode surface in two-electron reduction at potentials lower than −50 mV versus Ag/AgCl. However, we have never observed noticeable catalytic currents in the absence of H_2O_2 at the same potentials when we immobilized HRP on screen printed electrodes in a thin nafion® film or within mesoporous materials likely because of slow oxygen reduction kinetics at our electrodes. Moreover, to our best knowledge, no publications reported the same behavior, which may mean that a specific electrode modification and electrode materials in work [19] could influence the results by unknown mechanism. In this work, we elaborated a completely

novel strategy to avoid addition of H_2O_2 based on the unique properties of titanium dioxide (TiO_2) to accumulate reactive oxygen species and play the role of hosting matrix for HRP.

Over the past two decades, TiO_2 based catalysts have received much attention for their applications [20], mainly because it is an environment-friendly material with good biocompatibility and stability [21, 22]. It has been shown that TiO_2 can adsorb and stabilize enzymes including HRP for the usage in removal and detection of phenolic pollutants [23, 24] that may occur in medical, food and environmental matrices [25]. It has been known for many years that the treatment of TiO_2 by H_2O_2 yields to complexation between titanium ions and H_2O_2 in a form of an active oxygen-donating intermediate that is active in oxidation reactions of organic compounds [26, 27]. Despite the known formation of reactive oxygen species (ROS) over H_2O_2-treated TiO_2, to our best knowledge, no publications exist regarding the application of this type of catalyst for the construction of biosensors.

The aim of this work is to explore the use of TiO_2 that generates ROS in the presence of H_2O_2. Herein, we report an original strategy for HRP-based biosensors that can work in solution containing no H_2O_2 and only need a short pre-activation of a TiO_2-HRP based electrode. Thus, such enzyme electrode works as a reagent-less sensor, *i.e.* can sense phenols and aromatic amines without adding a co-substrate in the measuring solution, which opens new opportunities for developing easy-to-use on-site tests.

2. Experimental

2.1. Materials

Hydrogen peroxide (H_2O_2, 35 wt%), nafion® 117 (5% in a mixture of lower aliphatic alcohols and water), potassium chloride (KCl), 4-aminophenol (4AP, 98+%), silicon dioxide (SBA-15, mesoporous), and potassium phosphate monobasic (KH_2PO_4) were purchased from Sigma-Aldrich. Hydroquinone (HQ, 99.5%) was purchased from Acros, and TiO_2 (Millennium PC500, mesoporous) was obtained from Crystal Global. Prior to use, TiO_2 was calcined to 450 °C to enlarge its pore size [28]. Horseradish peroxidase (HRP, EC 1.11.1.7, activity 293 U/mg) was purchased from Calbiochem. The measuring buffer contained 0.01 M phosphate at pH 7 and 0.1 M KCl as supporting electrolyte. All reagents were used without further purification and all solutions were prepared with deionized water.

2.2. Apparatus

Electrochemical measurements were carried out using PalmSens (Utrecht, The Netherlands) with PSTrace software (version 3.0). Experiments in the presence of HQ were conducted in a conventional three-electrode electrochemical cell (10 mL) using a saturated calomel electrode (SCE) and a glassy carbon rod as a reference and a counter electrode, respectively. A carbon screen-printed electrode (SPE, ItalSens) was used as working electrode. 4AP and other tested phenols were measured in a droplet, *i.e.* by placing a drop of 100 μL onto a SPE. Since the potential of the screen-printed Ag quasi-reference electrode in the measuring buffer was ca. +0.04 V versus SCE, the amperometric measurements in a droplet were conducted at a potential of −0.14 V which corresponded −0.1 V versus SCE.

UV-vis were recorded in the range of 200-500 nm using a SYNERGYTM MX (Biotek, USA). For EPR (electron paramagnetic resonance) measurements, X-band (~9.44 GHz) continuous-wave (CW) EPR experiments were performed on a Bruker ESP300E spectrometer equipped with a liquid Helium cryostat (Oxford Inc.). The EPR spectra were recorded at 2.5 K, with a modulation amplitude of 5 mT, a microwave power of 1 mW and a modulation frequency of 100 kHz. A vacuum pump was attached to the EPR sample tube to remove the excess paramagnetic oxygen from the sample during the experiments. All EPR spectra are presented normalized for facile comparison and are simulated using the MATLAB toolbox Easyspin [29].

2.3. Modification of the electrode

The procedure for immobilization of HRP in TiO_2 is reported elsewhere [30]. Briefly, 20 mg TiO_2 was added to 0.25 mL of 66 μM HRP in 10 mM HEPES pH 7 and incubated for 18 h at a rotary shaker at room temperature. After this stage, 95% of the total amount of HRP was adsorbed onto TiO_2 as measured by UV-vis of the supernatant that results in 3.4 wt% HRP in the TiO_2-HRP powder. Similarly, we estimated that the maximal loading reaches 4.7 wt% at higher concentrations of HRP (Table S1). Finally, the resulting powder (TiO_2-HRP) was filtered through a millipore 0.45 μm filter, washed with excess of pure buffer, and dried and then stored at +4 °C.

To modify a SPE, a suspension (5 μL) consisting of TiO_2-HRP (10 mg/ml) and nafion® (5% in a mixture of lower aliphatic alcohols and water) in 10 mM HEPES pH 7 was dropped on the surface of the working electrode of the SPE and dried at room temperature for approximately 1 h. The modified electrodes were abbreviated as SPE|TiO_2-HRP. To identify the role of TiO_2, SiO_2 (SBA-15) impregnated with HRP was prepared and drop-casted on a SPE in the same

way. These electrodes were abbreviated as SPE|SiO_2-HRP. For the pre-incubation tests, the modified electrodes were incubated for 2 min in 1 mM H_2O_2 solution and carefully washed in copious amount of the pure buffer.

2.4. UV-vis determination of HQ oxidized by TiO_2-HRP after activation in H_2O_2

For activation, 1 mg of TiO_2-HRP was incubated in 1 mL of 1 mM H_2O_2 for 5 min. Next, the suspension was centrifuged at 14000 rpm for 1 min and the supernatant was discharged. The precipitated TiO_2-HRP was washed with 1 mL phosphate buffer and centrifuged again. This washing step was repeated three times. Finally, the activated and washed TiO_2-HRP was re-suspended in 1 mL of 25 µM HQ in the phosphate buffer and incubated for 1 h in dark. The UV-vis spectra of HQ before incubation with TiO_2-HRP and the supernatant after incubation with activated TiO_2-HRP were recorded and the amount of HQ oxidized was calculated from the decrease in the absorbance band of HQ at 288 nm.

3. Results and discussion

3.1. The feasibility of avoiding H_2O_2 in HRP based sensing

Peroxidases, *e.g.* HRP, catalyse the oxidation of a wide range of phenols and aromatic amines by H_2O_2 and, thus, peroxidases were employed in numerous second and third generation electrochemical biosensors [17, 31-34]. For the detection of phenolic compounds by a HRP-based sensor, an analyte undergoes redox cycling between the enzyme (oxidation) and a polarized electrode (reduction) while H_2O_2 plays a role of the sacrificial electron acceptor for HRP (Fig. 1A) [35-37]. However, H_2O_2 is an electroactive compound and its addition into the measuring buffer causes a large spike in the background current followed by continuous background drift (Fig. 1C). Consequently, additional time is needed to stabilize the background drift to an acceptable level. These issues become even more daunting when conducting measurements are performed in a droplet because of poor repeatability of the background drift induced by H_2O_2 addition. Obviously, a strategy that can avoid direct addition of H_2O_2 in the measuring buffer, is advantageous and desirable.

In this work, we suggest incubation of SPE|TiO_2-HRP in 1 mM H_2O_2 for a short time in order to pre-activate. Afterwards, the electrodes were rinsed with a copious amount of pure buffer to remove excess and weakly adsorbed H_2O_2 and tested in the electrochemical cell containing the working buffer without H_2O_2. In the following text these electrodes are abbreviated as SPE|TiOOH-HRP in contrast to their non-activated versions SPE|TiO_2-HRP. The activity of

SPE|TiOOH-HRP was measured in the presence of HQ by recording a reduction current of benzoquinone (BQ) formed in the HRP-catalyzed enzymatic reaction, *i.e.* in a similar way as if H_2O_2 would be present in the solution (Fig. 1B). Surprisingly, SPE|TiOOH-HRP showed intense responses to HQ in the range of 0.05 – 2 μM (Fig. 1D, Fig. S1), with values that were even higher than the responses at SPE|TiO_2-HRP obtained in the presence of 1 mM H_2O_2.

Comparative behaviour of SPE|TiOOH-HRP and SPE|TiO_2-HRP during amperometric measurements of HQ, our model analyte, is shown in Fig. 1C and D. A large spike and a considerably long background stabilization time (*ca.* 600 s) was observed in case of SPE|TiO_2-HRP after adding H_2O_2 (Fig. 1C), while the background current at SPE|TiOOH-HRP was stable from the onset of the amperometric experiment (Fig. 1D). Furthermore, at sub-μM concentrations (0.05-1 μM) SPE|TiOOH-HRP showed a sensitivity of 3.04 ± 0.15 A M^{-1} cm^{-2} (average ± SD from three independent experiments) which is six times higher than the sensitivity observed at SPE|TiO_2-HRP, operating in the presence of 1 mM H_2O_2, 0.54 ± 0.05 A M^{-1} cm^{-2}. However, the current-concentration curve levels out already at 2 μM for SPE|TiOOH-HRP and at only 40 μM for SPE|TiO_2-HRP operated in the presence of H_2O_2. In other words, SPE|TiOOH-HRP outperforms in the low concentration range (0.05 – 2 μM), but gives a comparatively lower response at higher concentrations (> 2 μM). This is not an issue for the detection of phenolic contaminants, which should be normally monitored in the sub-μM concentration range.

The sensitivity of the pre-activated electrode (SPE|TiOOH-HRP) towards HQ in the solution containing no H_2O_2 can be explained by the accumulation of the hydroperoxyl functionalities (-OOH) created on the surface of the activated electrode during the pre-activation step [38]. These functionalities may further release reactive oxygen species that interact with the adsorbed HRP. We also exclude comparatively weak physical adsorption of H_2O_2 on the TiO_2 surface because the electrodes kept their ability to oxidize phenolic compounds during a period of *ca.* twenty minutes, even after vigorous washing and being placed in a large volume (10 mL) of pure buffer solution.

The formation of hydroperoxyl functionalities can occur on TiO_2 but not on SiO_2. Thus, to further emphasize the role of TiO_2, an electrode modified by SiO_2-HRP (SPE|SiO_2-HRP) was prepared and pre-activated by a H_2O_2 solution. However, no electrochemical responses could be observed upon adding HQ (Fig. 1D inset) meaning that the activation effect is only observed for TiO_2. In contrast, after adding 1 mM H_2O_2 in the cell solution, SPE|SiO_2-HRP gave similar

responses to HQ as it was observed at SPE|TiO_2-HRP with H_2O_2 being present in the measuring cell (Fig. S2). This suggests that SPE|SiO_2-HRP contained the same amount of active HRP molecules, but it could not be activated by a short incubation in H_2O_2 as it is the case for TiO_2-based electrodes. The result supports the hypothesis of the formation of hydroperoxyl functionalities.

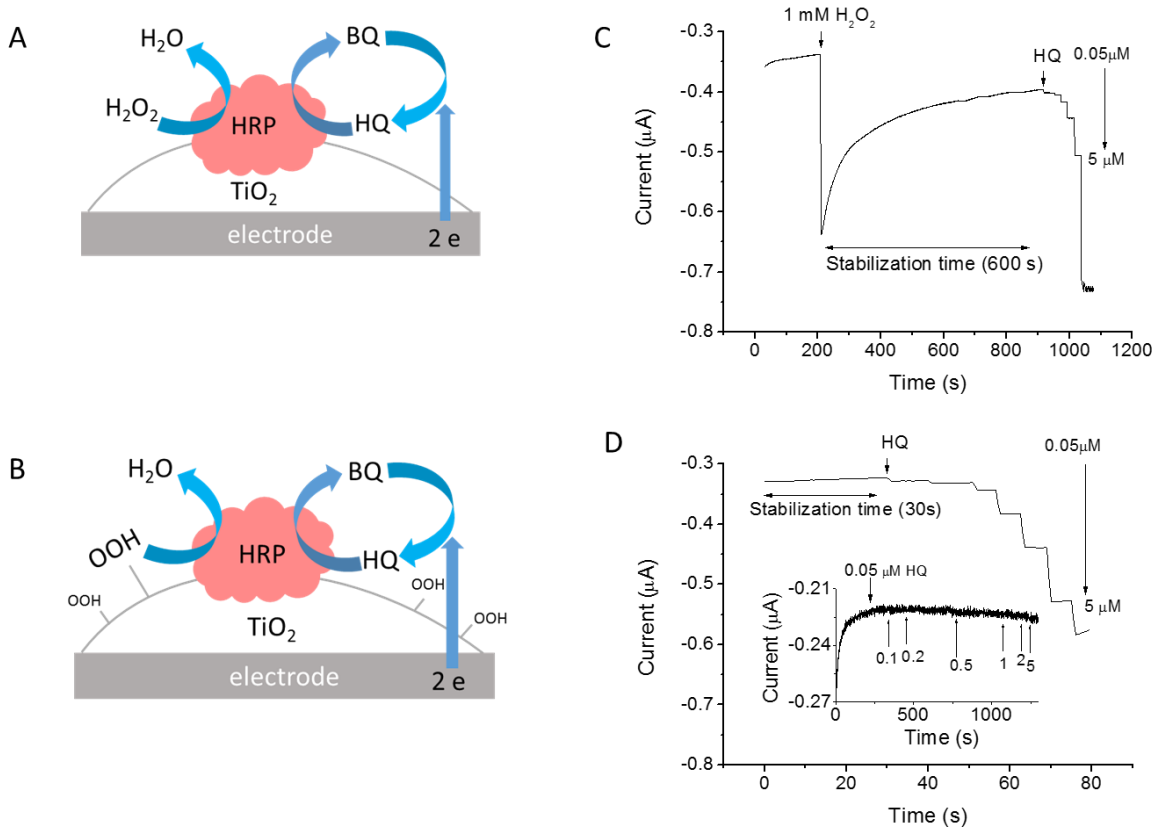

Figure 1. Comparison of the reaction mechanism and amperometric behaviour of two detection schemes. (A) The HRP reaction mechanism in the presence of H_2O_2 in solution and (B) at a pre-activated Ti-OOH electrode. (C) The baseline fluctuation after the addition of 1 mM H_2O_2 and amperometric detection HQ at SPE|TiO_2-HRP. (D) Detection of HQ at SPE|TiOOH-HRP. Inset: Amperometric responses at a pre-activated SPE|SiO_2-HRP. The number denote the concentration of HQ (μM). Measuring buffer, 0.01 M phosphate buffer (pH 7.0) containing 0.1 M KCl. Applied potential, -0.10 V vs. SCE.

3.2. EPR and UV-vis characterization

To study the functionalities created at the TiO_2 surface after contact with H_2O_2, EPR analysis was performed. Initially, blank TiO_2 (without HRP) in 10 mM HEPES buffer pH 7 was measured by EPR and subsequently 10 mM H_2O_2 was added, followed by another EPR measurement. By subtracting the EPR spectrum of blank TiO_2 from the latter, the resulting anisotropic EPR spectrum shown in Fig. 2A is obtained.

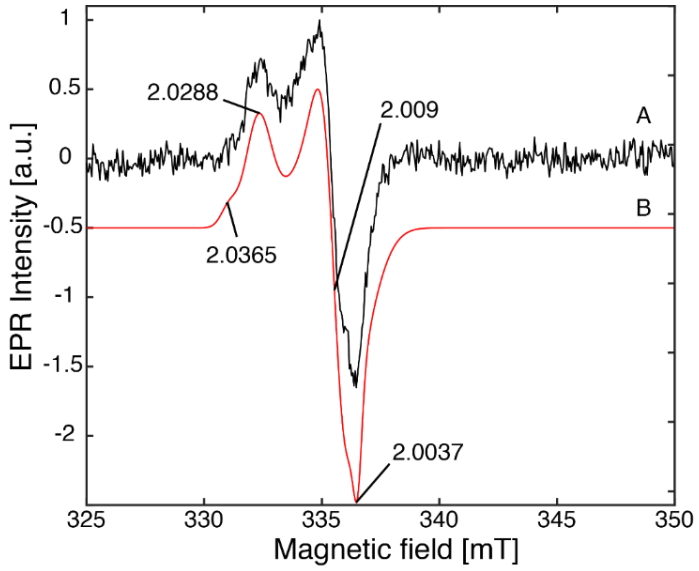

Figure 2. CW-EPR spectrum of (A) the subtraction of the EPR spectrum of TiO_2 + H_2O_2 from the EPR spectrum of TiO_2 and (B) the corresponding simulation.

Simulations (Fig. 2B) reveal *g*-values of g_z = 2.0288 (±0.0002), g_y = 2.0090 (±0.0002) and g_x = 2.0037 (±0.0002). These values are ascribed to the superoxide anion O_2^- bound on the Ti^{4+}-centers [39-43]. Another weak signal is observed due to a second O_2^- with g_z = 2.0365. The two O_2^- signals show the same g_y and g_x values. The difference in g_z component originates from the differences in crystal field due to the different location of O_2^- on TiO_2 surface [40, 42, 44, 45]. It is suggested that through homolysis of H_2O_2 to HO• radicals the side reaction occurs: [39, 41]

$$H_2O_2 \longrightarrow 2HO\bullet \xrightarrow{Ti} Ti\text{-}OOH$$

This further leads to the formation of O_2^- due to the reaction of the -OOH functionalized TiO_2 with hydroxyl radicals. No such effect was found for silica treated with H_2O_2 (Fig. S3). The full EPR spectra of non-activated and H_2O_2-activated TiO_2-HRP are shown in Fig. S4. In the 100-150 mT region of Fig. S4A, the low-field component of the high-spin ferric forms of HRP are observed. A multitude of components is seen, in line with earlier observations for peroxidases that show that the heme pocket is very heterogeneous [46]. By adding H_2O_2, many components of this signal disappear, in line with the expected two-electron oxidation to compound I, which is an oxoferryl iron (Fe^{4+}=O) and a porphyrin π cation radical [47, 48]. The amount of HRP compound I depends on the amount of H_2O_2 added [47]. In this case a high amount of H_2O_2 (10 mM) is used to investigate the influence of H_2O_2 on both the enzyme and TiO_2. Figure S5 zooms into the region where radical contributions are expected for TiO_2-HRP in HEPES buffer (Fig. S5A) and activated TiO_2-HRP (Fig. S5B). The difference between spectrum S5B and S5A is

shown in Figure S5C. Besides contributions of O_2^- radicals as observed for TiO_2 treated with H_2O_2 (Fig. 2), an extra radical signal stemming from the porphyrin radical of compound I is observed (indicated with red dashed line). By raising the temperature above 20 K, the radical signal could not be observed anymore in line with what is expected for a compound I porphyrin radical [47].

To estimate the amount of reactive oxygen species accumulated in the pre-activation step on TiO_2-HRP, we measured the amount of HQ that can be oxidized by TiO_2-HRP after treatment by 1 mM H_2O_2 for 5 min and vigorous washing with pure buffer. UV-vis spectra of the HQ solution were recorded before and after 1 h incubation with pre-activated TiO_2-HRP. Absorbance of HQ peak at 288 nm decreased after the incubation while a new band attributed to BQ, appeared at 245 nm. Since the absorbance bands of HQ and BQ do not overlay noticeably, we could calculate the amount of HQ oxidized in the experiment through the relative change in the absorbance at 288 nm. In average, 12.8 ± 1.4 nmol HQ was oxidized by 1 mg activated TiO_2-HRP that corresponds to 12.8 µmol/g accumulated ROS as a H_2O_2 equivalent. As a control, similar experiments were performed with non-activated TiO_2-HRP and pre-activated SiO_2-HRP and TiO_2 that resulted in only negligible values of oxidized HQ (Table 1).

Table 1. Amounts of HQ oxidized at the surface of different matrices pre-activated in 1 mM H_2O_2 in comparison with non-activated ones as calculated from the UV-vis spectrometry measurements.

Material	**Amount of HQ oxidized ± SD (µmol/g)**
TiO_2-HRP (pre-activated)	12.8 ± 1.4
TiO_2-HRP (non-activated)	1.3 ± 0.3
TiO_2 (pre-activated)	1.2 ± 0.2
SiO_2-HRP (pre-activated)	0.0 ± 0.0

3.3. Sensitivity and operational stability

To study the effect of the enzyme loading, TiO_2 was impregnated with different amounts of HRP (Table S1). A maximal loading of 1.06 µmol HRP per g TiO_2 (4.7 wt%) was determined by UV-vis from the change of HRP concentration in the supernatant after incubation of TiO_2 in HRP solutions of different volumes. The sensitivity of the electrodes increased linearly with the loading of HRP, for both SPE|TiO_2-HRP with H_2O_2 in the cell solution and SPE|TiOOH-HRP. Clearly, for all loadings the sensitivity was higher in the case of the pre-activated electrodes. However, the operational stability of the pre-activated electrode with the highest

loading was the worst: the electrode had only 56% of its activity after 30 min in 0.5 µM HQ (Fig. S6). The electrode with a loading of 0.77 µmol/g kept 80% activity in the same conditions and the electrodes with this loading were used in all further experiments.

3.4. Effect of the incubation time of the pre-activation step

Variation of the time of the pre-activation step revealed that even a short two minute incubation is sufficient to activate the electrode surface, while the sensitivity gradually decreased with the treatment time, probably due to some inactivation of the enzyme (Fig. S7). As a result, a pre-treatment time of 2 min was selected for all measurements.

Interestingly, SPE|TiO_2-HRP gives a minor response (*ca.* 70 nA) even without pre-activation in H_2O_2 (black square in Fig. S7). The most probable explanation is that TiO_2 may accumulate reactive oxygen species in small amounts without treatment by H_2O_2 due to generated the electron-hole pair upon exposure to ambient day light. It is known that the excited-state electrons and holes after reaction with water and oxygen can produce and accumulate reactive oxygen species [49, 50] similarly to the activation step with H_2O_2 but in comparatively small amounts that resulted in a lower sensitivity to HQ.

3.5. Effect of working potential

The sensitivity of the electrodes is influenced by the working potential of the amperometric detections. The dependence was investigated over a potential range from 0.1 to -0.4 V in a solution containing 1 µM HQ (Fig. S8). The response of the pre-activated electrodes proportionally increased as the applied potential shifted towards more negative values reaching a plateau at -0.3 V. At more negative potential values, the electrochemical reduction of molecular oxygen contributes considerably to the response of the phenolic compound and it may cause a slow irreversible deactivation of adsorbed HRP [51]. A low background current and no influence of oxygen reduction motivates the selection of a working potential of −0.10 V.

3.6. Applicability of the SPE|TiOOH-HRP electrode

The amperometric response of SPE|TiOOH-HRP was monitored for different phenolic compounds and referred to the current response obtained in the presence of HQ (Table S2). The trend of the reactivity can be explained by the nature of the phenolic structures, the position of the functionalities, and the ability of the substituents to form electron-donor conjugation [52, 53]. Among the phenolic substrates tested, HQ shows the highest sensitivity and reactivity

followed by 2-aminophenol (2AP), quercetin and 4-aminophenol (4AP). In the case of quercetin, 2AP, caffeic acid and 4AP, a corresponding conjugated structure is easily formed due to strong electron-donor conjugation of the substituents meaning that the free electron on the resulting quinone radical is stabilized by the charge distribution through the conjugated system [54, 55].

To explore the applicability of the SPE|TiOOH-HRP electrodes for on-site applications, 100 μL of 4AP solution was placed onto the SPE and the amperometric response was measured at a potential of -0.14 V (-0.10 V vs SCE) as shown in Fig. 3. Among the phenolic pollutants, 4-aminophenol (4AP) has industrial relevance due to its occurrence as an intermediate in the synthesis of pharmaceuticals [56] or as a stain for wood, fur and feathers [57]. 4AP was also identified as a degradation product of paracetamol, therefore it is frequently present in paracetamol tablet formulation and wastewater [58, 59].

The calibration plot exhibits a typical current response of the electrode with increasing 4AP concentration (Fig. 3B). The concentration-response profile (Fig. 3B) for SPE/TiOOH-HRP was near linear in the concentration range 0.025 – 1 μM and saturated at 2 – 5 μM. The average sensitivity ± SD (three different electrodes) was 2.73 ± 0.99 A M^{-1} cm^{-2} and the limit of detection was 24 nM. The detection limit for 4-AP in the present work is at least two times lower than reported in the literature for other biosensors (Table S3) which indicates favourable analytical performance of our electrochemical biosensor.

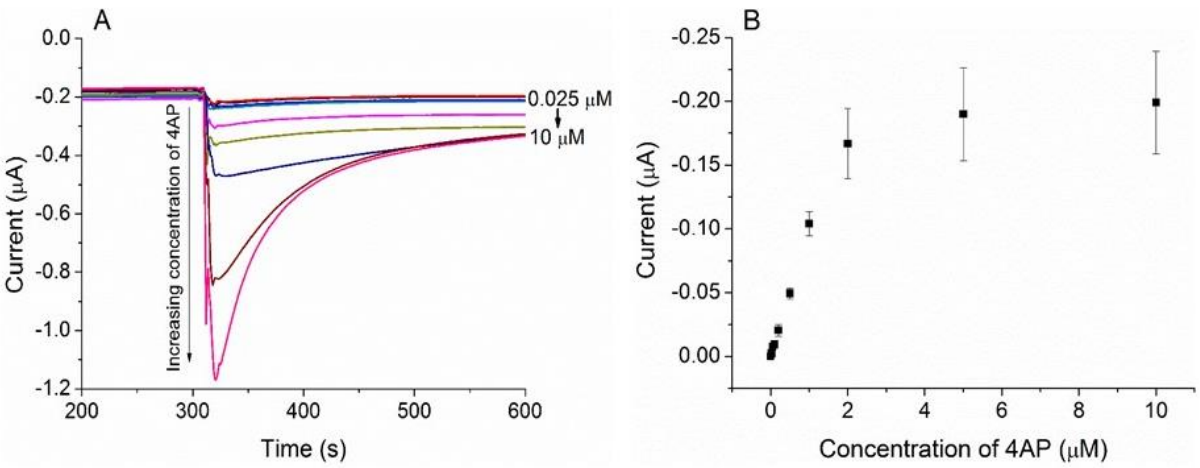

Figure 3. Chronoamperometry curves (A) and calibration plot (B) obtained for 4-aminophenol at SPE|TiOOH-HRP in 0.01 M phosphate buffer (pH 7.0) containing 0.1 M KCl. Applied potential, -0.14 V (-0.1 V vs SCE).

4. Conclusion

For the first time we show that TiO_2 can accumulate reactive oxygen species allowing it to act as sacrificial electron acceptor for HRP when an analyte undergoes redox cycling between enzymatic oxidation by HRP and electrochemical reduction at an electrode. The amount of species accumulated after a short pre-activation step in H_2O_2 and followed washing was enough to support the response of electrodes in the range of concentration up to 2-5 μM. Applying the pre-activation step instead of adding H_2O_2 in the measuring buffer improves the background stability and LOD in amperometric detection of phenols compared to the conventional HRP-based electrosensing strategy. EPR spectroscopy revealed the presence of O_2^- at the surface of TiO_2 after the pre-activation step.

The proposed detection scheme goes beyond the traditional concept of both second and third generation biosensors suggesting a new direction for the development of enzymatic sensors based on redox cycling and a surface confined sacrificial electron acceptor. This approach simplifies the analysis and gives possibilities for a straightforward design of sensors to detect a wide range of phenolic pollutants.

Acknowledgement

The authors thank the University of Antwerp (GOA) and the Fund for Scientific Research-Flanders (FWO) (grant 12T4219N) for funding. V. Rahemi is financially supported through a postdoctoral fellowship of the Research Foundation–Flanders (FWO).

Appendix A. Supplementary data

Supplementary data associated with this article can be found in the online version.

References

[1] L.G.C. Villegas, N. Mashhadi, M. Chen, D. Mukherjee, K.E. Taylor, N. Biswas, A Short Review of Techniques for Phenol Removal from Wastewater, Current Pollution Reports, 2(2016) 157-67.
[2] M.M. William Wilson Anku, Penny Govender, Phenolic Compounds in Water: Sources, Reactivity, Toxicity and Treatment Methods, in: Mariana Palma Tenango, Marcos Soto-Hernandez, M.R. Garcia-Mateos (Eds.), Phenolic Compounds - Natural Sources, Importance and Applications, InTechOpen2017, pp. 419-43.
[3] X. Sun, C. Wang, Y. Li, W. Wang, J. Wei, Treatment of phenolic wastewater by combined UF and NF/RO processes, Desalination, 355(2015) 68-74.
[4] F. Chekin, L. Gorton, I. Tapsobea, Direct and mediated electrochemistry of peroxidase and its electrocatalysis on a variety of screen-printed carbon electrodes: amperometric hydrogen peroxide and phenols biosensor, Anal Bioanal Chem, 407(2015) 439-46.
[5] I.G. Gazaryan, L. Gorton, T. Ruzgas, E. Csoregi, W. Schuhmann, L.M. Lagrimini, et al., Tobacco peroxidase as a new reagent for amperometric biosensors, J Anal Chem, 60(2005) 558-66.
[6] P. Önnerfjord, J. Emnéus, G. Marko-Varga, L. Gorton, F. Ortega, E. Domínguez, Tyrosinase graphite-epoxy based composite electrodes for detection of phenols, Biosensors and Bioelectronics, 10(1995) 607-19.
[7] R.S. Freire, N. Durán, L.T. Kubota, Effects of fungal laccase immobilization procedures for the development of a biosensor for phenol compounds, Talanta, 54(2001) 681-6.
[8] A. Lindgren, J. Emnéus, T. Ruzgas, L. Gorton, G. Marko-Varga, Amperometric detection of phenols using peroxidase-modified graphite electrodes, Analytica Chimica Acta, 347(1997) 51-62.
[9] S. Yang, Y. Li, X. Jiang, Z. Chen, X. Lin, Horseradish peroxidase biosensor based on layer-by-layer technique for the determination of phenolic compounds, Sensors and Actuators B: Chemical, 114(2006) 774-80.
[10] B. Serra, B. Benito, L. Agüí, A.J. Reviejo, J.M. Pingarrón, Graphite-Teflon-Peroxidase Composite Electrochemical Biosensors. A Tool for the Wide Detection of Phenolic Compounds, Electroanalysis, 13(2001) 693-700.
[11] T. Ruzgas, J. Emnéus, L. Gorton, G. Marko-Varga, The development of a peroxidase biosensor for monitoring phenol and related aromatic compounds, Analytica Chimica Acta, 311(1995) 245-53.
[12] S.i. Imabayashi, Y.T. Kong, M. Watanabe, Amperometric Biosensor for Polyphenol Based on Horseradish Peroxidase Immobilized on Gold Electrodes, Electroanalysis, 13(2001) 408-12.
[13] N. Durán, E. Esposito, Potential applications of oxidative enzymes and phenoloxidase-like compounds in wastewater and soil treatment: a review, Applied Catalysis B: Environmental, 28(2000) 83-99.
[14] S. Trashin, V. Rahemi, K. Ramji, L. Neven, S.M. Gorun, K. De Wael, Singlet oxygen-based electrosensing by molecular photosensitizers, Nature Communications, 8(2017) 16108.
[15] F.-D. Munteanu, A. Lindgren, J. Emnéus, L. Gorton, T. Ruzgas, E. Csöregi, et al., Bioelectrochemical Monitoring of Phenols and Aromatic Amines in Flow Injection Using Novel Plant Peroxidases, Analytical Chemistry, 70(1998) 2596-600.
[16] V. Carralero, M.L. Mena, A. Gonzalez-Cortés, P. Yáñez-Sedeño, J.M. Pingarrón, Development of a high analytical performance-tyrosinase biosensor based on a composite graphite–Teflon electrode modified with gold nanoparticles, Biosensors and Bioelectronics, 22(2006) 730-6.
[17] S. Korkut, B. Keskinler, E. Erhan, An amperometric biosensor based on multiwalled carbon nanotube-poly(pyrrole)-horseradish peroxidase nanobiocomposite film for determination of phenol derivatives, Talanta, 76(2008) 1147-52.
[18] S.K. Ozoner, M. Yalvac, E. Erhan, Flow injection determination of catechol based on polypyrrole–carbon nanotube–tyrosinase biocomposite detector, Current Applied Physics, 10(2010) 323-8.
[19] S.C. Chang, K. Rawson, C.J. McNeil, Disposable tyrosinase-peroxidase bi-enzyme sensor for amperometric detection of phenols, Biosensors and Bioelectronics, 17(2002) 1015-23.
[20] J. Bai, B. Zhou, Titanium Dioxide Nanomaterials for Sensor Applications, Chemical reviews, 114(2014) 10131-76.

[21] R. Zhang, A.A. Elzatahry, S.S. Al-Deyab, D. Zhao, Mesoporous titania: from synthesis to application, Nano Today, 7(2012) 344-66.
[22] T. Rajh, N.M. Dimitrijevic, M. Bissonnette, T. Koritarov, V. Konda, Titanium dioxide in the service of the biomedical revolution, Chem Rev, 114(2014) 10177-216.
[23] S.S. Rosatto, L.T. Kubota, G. de Oliveira Neto, Biosensor for phenol based on the direct electron transfer blocking of peroxidase immobilising on silica–titanium, Anal Chim Acta, 390(1999) 65-72.
[24] J. Yu, H. Ju, Preparation of porous titania sol-gel matrix for immobilization of horseradish peroxidase by a vapor deposition method, Anal Chem, 74(2002) 3579-83.
[25] J. Zabicky, Analytical aspects of phenolic compounds, in: Z. Rappoport (Ed.) The Chemistry of Phenols, John Wiley & Sons New York, 2003, pp. 913-28.
[26] J.A. Connor, E.A.V. Ebsworth, Peroxy Compounds of Transition Metals, in: H.J. Emeléus, A.G. Sharpe (Eds.), Advances in Inorganic Chemistry and Radiochemistry, Academic Press1964, pp. 279-381.
[27] C. Prestipino, F. Bonino, S. Usseglio, A. Damin, A. Tasso, M.G. Clerici, et al., Equilibria between peroxo and hydroperoxo species in the titanosilicates: an in situ high-resolution XANES investigation, Chemphyschem : a European journal of chemical physics and physical chemistry, 5(2004) 1799-804.
[28] S. Ribbens, E. Beyers, K. Schellens, M. Mertens, X. Ke, S. Bals, et al., Systematic evaluation of thermal and mechanical stability of different commercial and synthetic photocatalysts in relation to their photocatalytic activity, Microporous Mesoporous Mater, 156(2012) 62-72.
[29] S. Stoll, A. Schweiger, EasySpin, a comprehensive software package for spectral simulation and analysis in EPR, J Magn Reson, 178(2006) 42-55.
[30] V. Rahemi, S. Trashin, V. Meynen, K. De Wael, An adhesive conducting electrode material based on commercial mesoporous titanium dioxide as a support for Horseradish peroxidase for bioelectrochemical applications, Talanta, 146(2016) 689-93.
[31] S. Xu, X. Zhang, T. Wan, C. Zhang, A third-generation hydrogen peroxide biosensor based on horseradish peroxidase cross-linked to multi-wall carbon nanotubes, Microchim Acta, 172(2011) 199-205.
[32] S.-X. Xu, J.-L. Li, Z.-L. Zhou, C.-X. Zhang, A third-generation hydrogen peroxide biosensor based on horseradish peroxidase immobilized by sol-gel thin film on a multi-wall carbon nanotube modified electrode, Anal Methods, 6(2014) 6310-5.
[33] X. Zeng, X. Li, X. Liu, Y. Liu, S. Luo, B. Kong, et al., A third-generation hydrogen peroxide biosensor based on horseradish peroxidase immobilized on DNA functionalized carbon nanotubes, Biosens Bioelectron, 25(2009) 896-900.
[34] S. Xu, B. Peng, X. Han, A third-generation H_2O_2 biosensor based on horseradish peroxidase-labeled Au nanoparticles self-assembled to hollow porous polymeric nanopheres, Biosens Bioelectron, 22(2007) 1807-10.
[35] M. Dequaire, B. Limoges, J. Moiroux, J.-M. Savéant, Mediated electrochemistry of horseradish peroxidase. Catalysis and inhibition, J Am Chem Soc, 124(2002) 240-53.
[36] J. Huang, E.M. Sommers, D.B. Kim-Shapiro, S.B. King, Horseradish peroxidase catalyzed nitric oxide formation from hydroxyurea, J Am Chem Soc, 124(2002) 3473-80.
[37] Y. Xianyu, Y. Chen, X. Jiang, Horseradish peroxidase-pediated, iodide-catalyzed cascade reaction for plasmonic immunoassays, Anal Chem, 87(2015) 10688-92.
[38] S. Bordiga, A. Damin, F. Bonino, G. Ricchiardi, C. Lamberti, A. Zecchina, The structure of the peroxo species in the TS-1 catalyst as investigated by resonant Raman spectroscopy, Angew Chem, Int Ed, 41(2002) 4734-7.
[39] F. Geobaldo, S. Bordiga, A. Zecchina, E. Giamello, G. Leofanti, G. Petrini, DRS UV-Vis and EPR spectroscopy of hydroperoxo and superoxo complexes in titanium silicalite, Catal Lett, 16(1992) 109-15.
[40] A. Tuel, J. Diab, P. Gelin, M. Dufaux, J.-F. Dutel, Y.B. Taarit, EPR evidence for the isomorphous substitution of titanium in silicalite structure, J Mol Catal, 63(1990) 95-102.
[41] D. Srinivas, P. Manikandan, S.C. Laha, R. Kumar, P. Ratnasamy, Reactive oxo-titanium species in titanosilicate molecular sieves: EPR investigations and structure – activity correlations, J Catal, 217(2003) 160-71.

[42] Q. Zhao, X.-h. Bao, Y. Wang, L.-w. Lin, G. Li, X.-w. Guo, et al., Studies on superoxide O_2^- species on the interaction of TS-1 zeolite with H_2O_2, J Mol Catal A: Chem, 157(2000) 265-8.
[43] J. Green, E. Carter, D.M. Murphy, An EPR investigation of acetonitrile reactivity with superoxide radicals on polycrystalline TiO_2, Res Chem Intermed, 35(2009) 145-54.
[44] G. Bellussi, M.S. Rigutto, Metal Ions Associated to the Molecular Sieve Framework: Possible Catalytic Oxidation Sites, in: J.C. Jansen, M. Stöcker, H.G. Karge, J. Weitkamp (Eds.), Studies in Surface Science and Catalysis, Elsevier1994, pp. 177-213.
[45] D. M. Murphy, E. W. Griffiths, C. C. Rowlands, D. M. Murphy, F. E. Hancock, E. Giamello, EPR study of the H_2O_2 interaction with TiO_2; evidence for a novel $S = 1$ surface radical pair, Chem Commun, (1997) 2177-8.
[46] D.A. Svistunenko, J.A.R. Worrall, S.B. Chugh, S.C. Haigh, R.A. Ghiladi, P. Nicholls, Ferric haem forms of Mycobacterium tuberculosis catalase-peroxidase probed by EPR spectroscopy: Their stability and interplay with pH, Biochimie, 94(2012) 1274-80.
[47] R. Aasa, T. Vänngård, H.B. Dunford, EPR studies on compound I of horseradish peroxidase, Biochim Biophys Acta, Enzymol, 391(1975) 259-64.
[48] M. Tanaka, K. Matsuura, S. Yoshioka, S. Takahashi, K. Ishimori, H. Hori, et al., Activation of hydrogen peroxide in horseradish peroxidase occurs within ∼200 μs observed by a new freeze-quench device, Biophys J, 84(2003) 1998-2004.
[49] A. Fujishima, T.N. Rao, D.A. Tryk, Titanium dioxide photocatalysis, J Photochem Photobiol, C, 1(2000) 1-21.
[50] H. Kisch, Semiconductor photocatalysis — mechanistic and synthetic aspects, Angew Chem, Int Ed, 52(2013) 812-47.
[51] E. Csöregi, G. Jönsson-Pettersson, L. Gorton, Mediatorless electrocatalytic reduction of hydrogen peroxide at graphite electrodes chemically modified with peroxidases, J Biotechnol, 30(1993) 315-37.
[52] Y.-C. Tsai, C.-C. Chiu, Amperometric biosensors based on multiwalled carbon nanotube-Nafion-tyrosinase nanobiocomposites for the determination of phenolic compounds, Sens Actuators, B, 125(2007) 10-6.
[53] S. Patai, The Chemistry of the Hydroxyl Group: Interscience Publishers; 1971.
[54] S.M. Yang, Y.M. Li, X.M. Jiang, Z.C. Chen, X.F. Lin, Horseradish peroxidase biosensor based on layer-by-layer technique for the determination of phenolic compounds, Sens Actuators, B, 114(2006) 774-80.
[55] X. Liu, L. Luo, Y. Ding, Y. Xu, Amperometric biosensors based on alumina nanoparticles-chitosan-horseradish peroxidase nanobiocomposites for the determination of phenolic compounds, Analyst, 136(2011) 696-701.
[56] S.J. Li, D.H. Deng, H. Pang, L. Liu, Y. Xing, S.R. Liu, Preparation of electrochemically reduced graphene oxide-modified electrode and its application for determination of p-aminophenol, J Solid State Electrochem, 16(2012) 2883-9.
[57] S. Mitchell, Kirk-Othmer Encyclopedia of Chemical Technology, Vol. II, fourth ed., New York: Wiley-Interscience; 1992.
[58] M.d.M. Gómez-Ramos, A. Pérez-Parada, J.F. García-Reyes, A.R. Fernández-Alba, A. Agüera, Use of an accurate-mass database for the systematic identification of transformation products of organic contaminants in wastewater effluents, J Chromatogr A, 1218(2011) 8002-12.
[59] M.S. Bloomfield, A sensitive and rapid assay for 4-aminophenol in paracetamol drug and tablet formulation, by flow injection analysis with spectrophotometric detection, Talanta, 58(2002) 1301-10.

Supplementary data

Enzymatic sensor for phenols based on titanium dioxide generating surface confined ROS after treatment with H_2O_2

Vanoushe Rahemi[a,b], Stanislav Trashin[a], Zainab Hafideddine[c], Vera Meynen[b], Sabine Van Doorslaer[c] and Karolien De Wael[a,*]

[a]*AXES research group, Department of Chemistry, University of Antwerp, Groenenborgerlaan 171, 2020 Antwerp, Belgium*

[b]*Laboratory of Adsorption and Catalysis (LADCA), Department of Chemistry, University of Antwerp, Universiteitsplein 1, B-2610 Wilrijk, Belgium*

[c]*Department of Physics, University of Antwerp, Universiteitsplein 1, B-2610 Wilrijk, Belgium*

[*]*Corresponding author. E-mail address: karolien.dewael@uantwerpen.be*

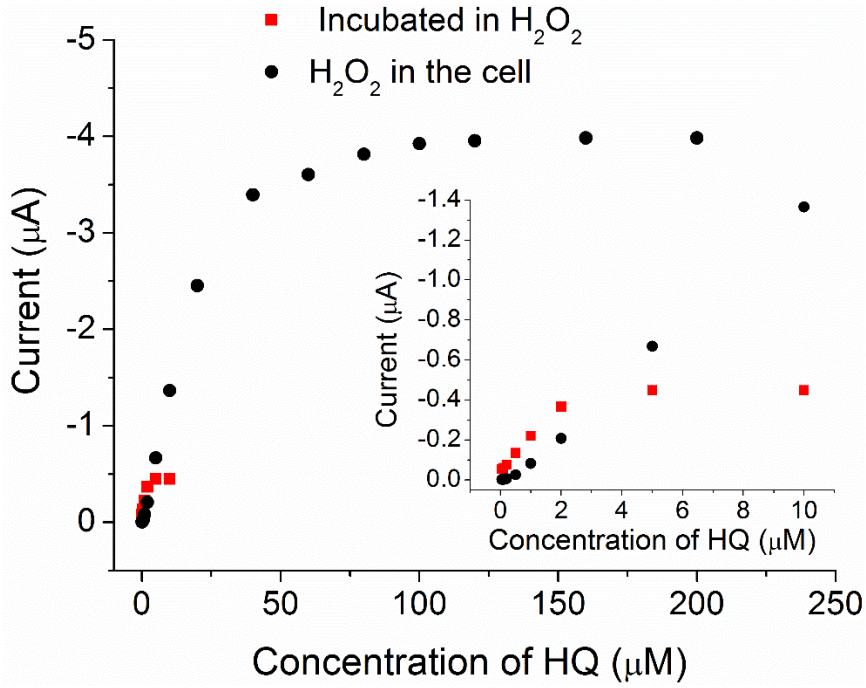

Figure S1. Calibration curve of SPE|TiOOH-HRP incubated for 2 min in 1 mM H_2O_2 (red) and SPE/ TiO_2-HRP used in the presence of 1 mM H_2O_2 (black). Inset: a lower HQ concentration range. Background electrolyte, 0.01 M phosphate buffer (pH 7.0) containing 0.1 M KCl. Applied potential, -0.10 V vs. SCE.

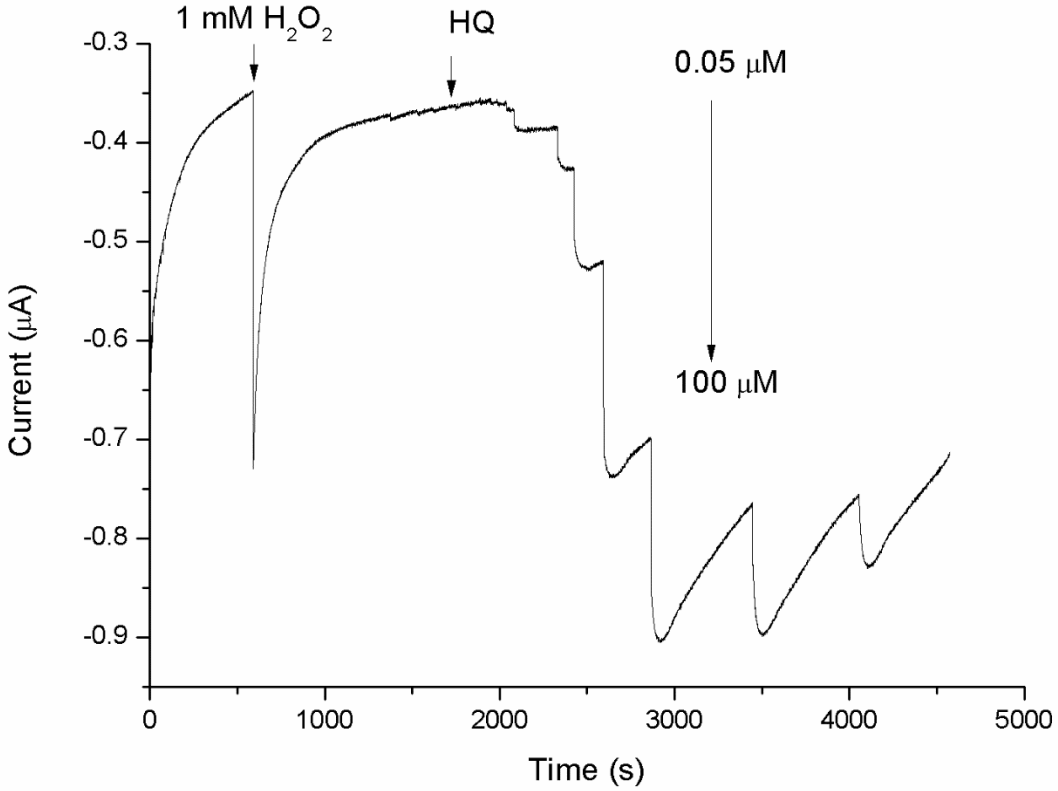

Figure S2. Amperometric responses at SPE|SiO_2-HRP towards different concentrations of HQ (μM) in the presence of 1 mM H_2O_2 in the measuring cell. Background electrolyte, 0.01 M phosphate buffer (pH 7.0) containing 0.1 M KCl. Applied potential, -0.10 V vs. SCE.

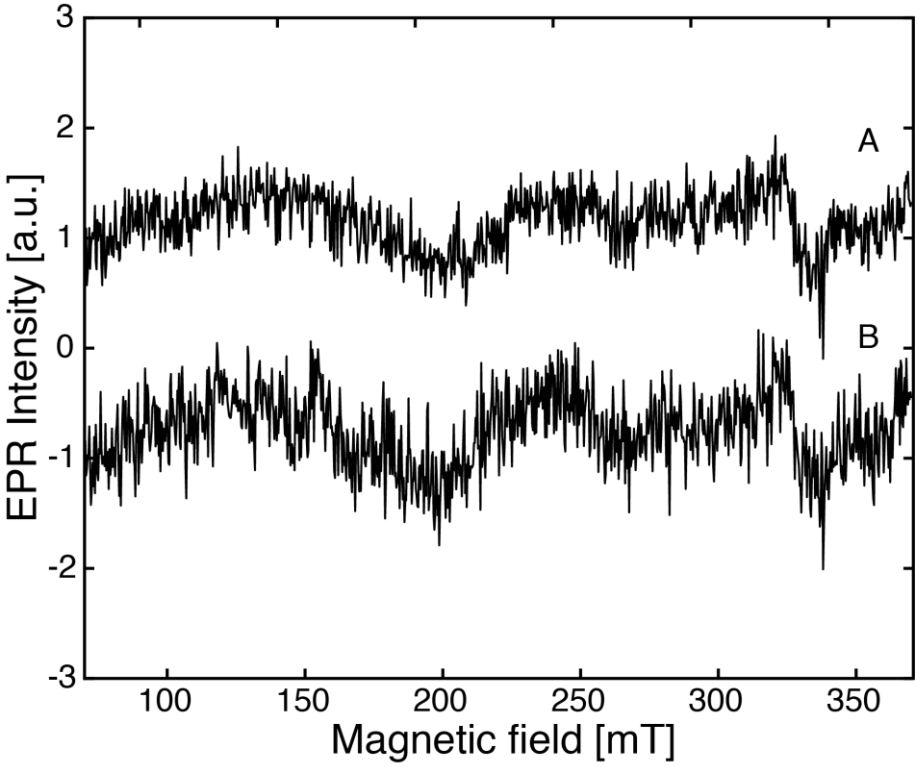

Figure S3. CW-EPR spectra of (A) SiO_2 in HEPES buffer and (B) SiO_2 with 10 mM H_2O_2.

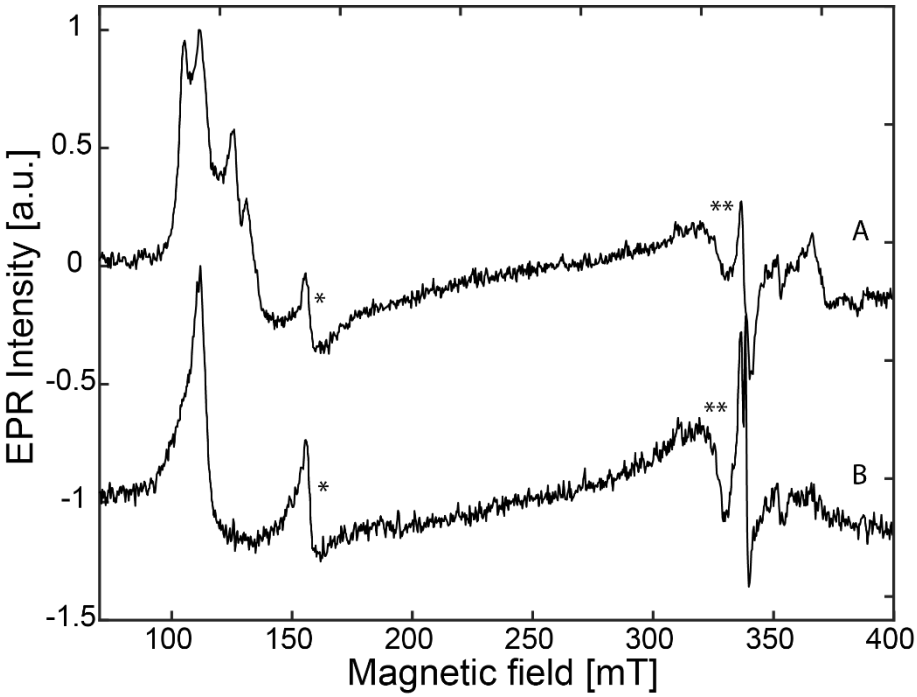

Figure S4. CW-EPR spectra of (A) TiO_2-HRP in HEPES buffer and (B) TiO_2-HRP with 10 mM H_2O_2. * indicates a non-heme iron signal and ** the Cu^{2+} background signal.

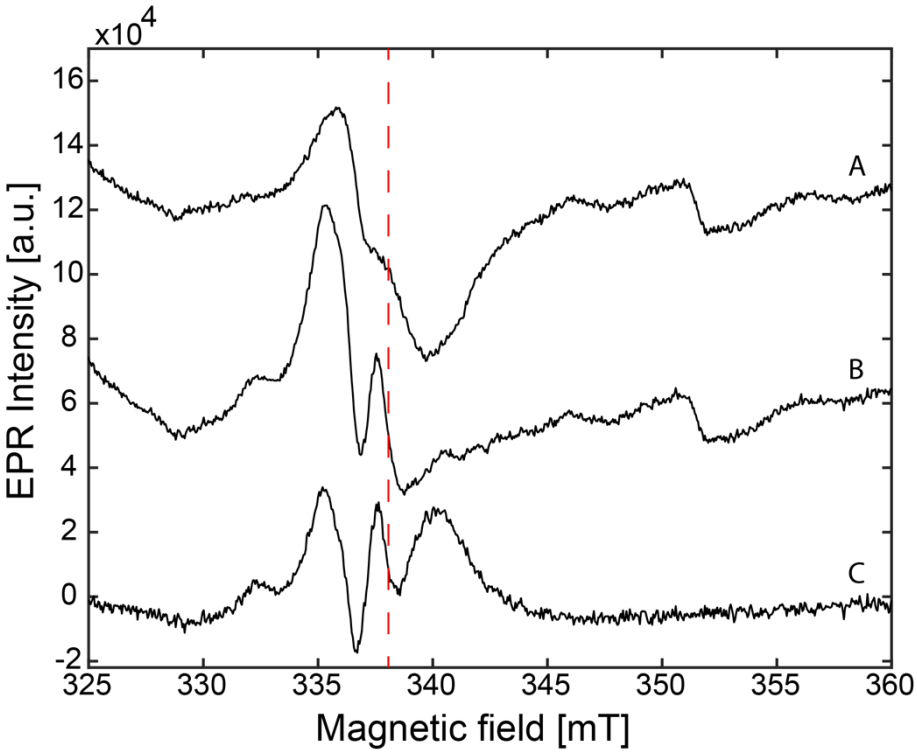

Figure S5. High-field CW-EPR spectra (not normalized) of (A) TiO_2-HRP in HEPES buffer, (B) TiO_2-HRP with 10 mM H_2O_2 and (C) difference spectrum (B)-(A). The position of the formed porphyrin π cation radical ($g \approx 2$) is indicated by the dashed line. The signal around 340 mT is possibly due to a Ti^{3+} component of the titania material.

Table S1. Dependence of the amperometric response on the amount of adsorbed HRP at SPE|TiOOH-HRP (after incubation for 2 min in 1 mM H_2O_2), compared to SPE|TiO_2-HRP in the presence of 1 mM H_2O_2 in the cell solution.

Loading (µmol/g)	Slope ± SD (nA/µM)	
	SPE|TiO_2-HRP in the presence of 1 mM H_2O_2	SPE|TiOOH-HRP in H_2O_2-free buffer
0.18	33.7 ± 1.4 (n=6)	60.0 ± 1.3 (n=6)
0.77	108 ± 15 (n=9)	150 ± 33 (n=10)
1.06	206 ± 15 (n=3)	295 ± 70 (n=3)

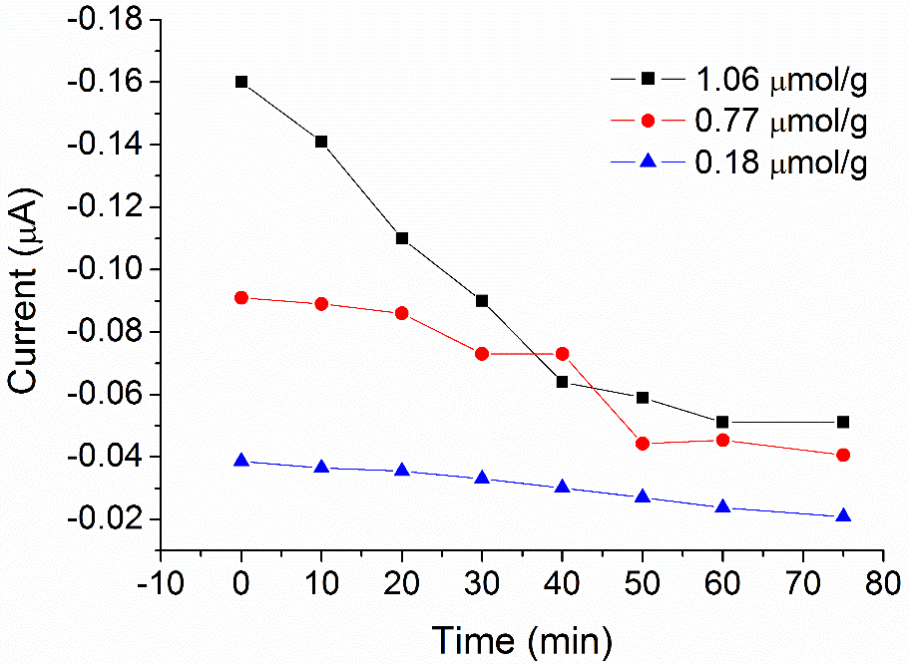

Figure S6. Stability of the response at SPE|TiOOH-HRP with different HRP loading in the presence of 0.5 μM HQ. The currents were recorded every 10 min. Background, 0.01 M phosphate buffer (pH 7.0) containing 0.1 M KCl. Applied potential, -0.10 V vs. SCE.

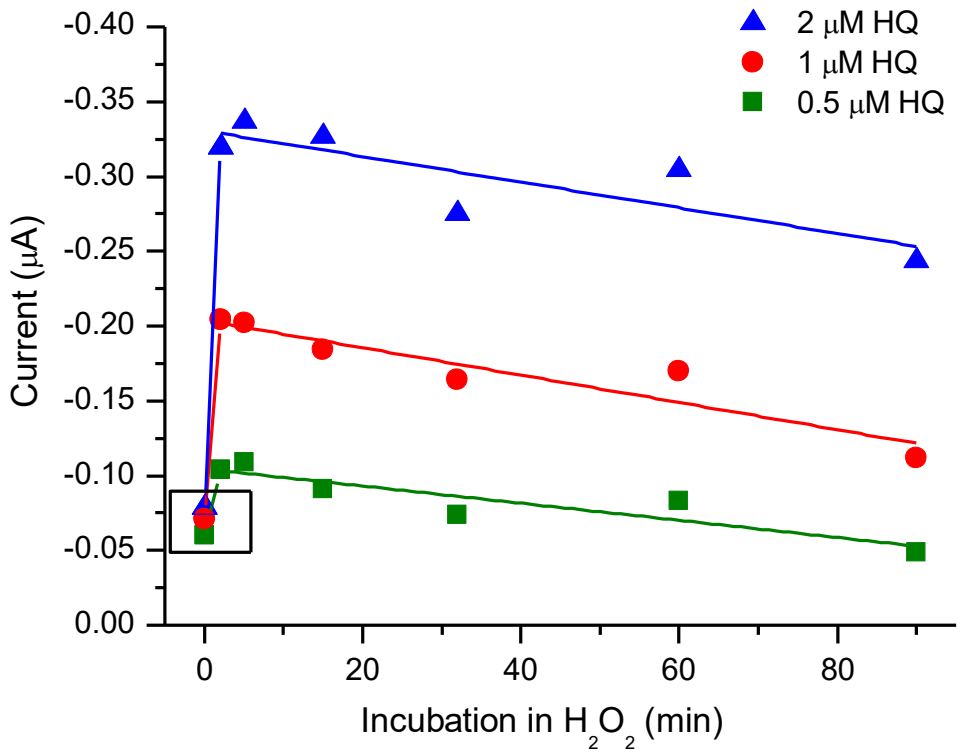

Figure S7. Effect of incubation time in 1 mM H_2O_2 on the response of SPE|TiOOH-HRP to three concentrations of HQ. Background, 0.01 M phosphate buffer (pH 7.0) containing 0.1 M KCl. Applied potential: -0.10 V vs. SCE.

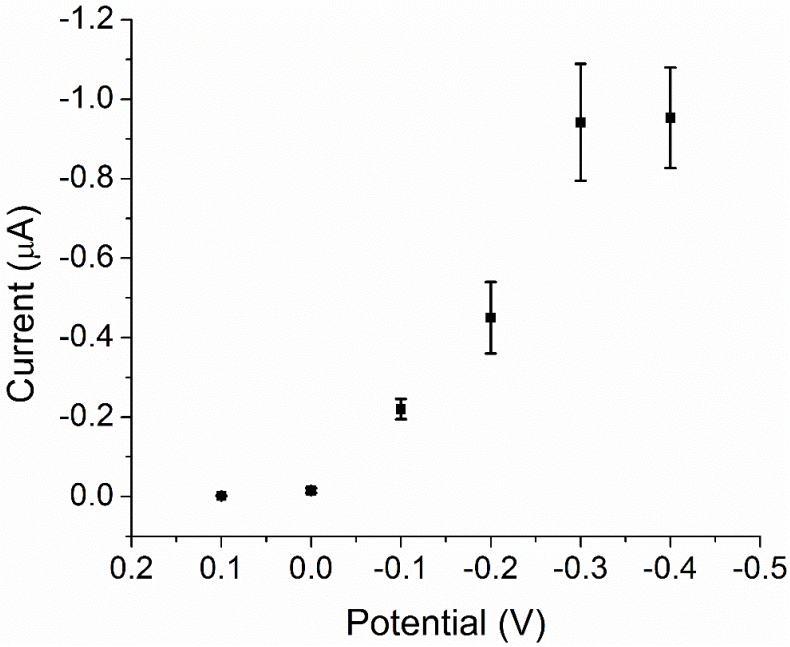

Figure S8. Influence of the applied potential on the amperometric response of 1 μM HQ at SPE|TiOOH-HRP in 0.01 M phosphate buffer (pH 7.0) containing 0.1 M of KCl.

Table S2. Responses of SPE|TiOOH-HRP to 2 μM phenolic compounds.Potential applied, -0.1 V vs. SCE.

Compound	Reduction current (nA)	Relative electrochemical activity (%)
HQ	-238	100
2-Aminophenol	-233	98
Quercetin	-170	71
Caffeic acid	-167	70
4-Aminophenol	-167	70
Catechol	-115	48
Phenol	-63	26

Table S3. Comparison of the detection limit for 4-aminophenol using different electrodes.

Electrode	**Limit of detection (μM)**
This method	0.024
Graphene-chitosan composite film modified glassy carbon electrode [1]	0.057
Graphene-polyaniline composite film modified electrode [2]	0.065
Carbon Ionic Liquid Electrode [3]	0.1
Single-wall carbon nanotube compound polymer film electrode [4]	0.06
Conductive copolymer-modified carbon fibre microelectrodes [5]	1

Referemces

[1] H. Yin, Q. Ma, Y. Zhou, S. Ai, L. Zhu, Electrochemical behavior and voltammetric determination of 4-aminophenol based on graphene–chitosan composite film modified glassy carbon electrode, Electrochimica Acta, 55(2010) 7102-8.
[2] Y. Fan, J.-H. Liu, C.-P. Yang, M. Yu, P. Liu, Graphene–polyaniline composite film modified electrode for voltammetric determination of 4-aminophenol, Sensors and Actuators B: Chemical, 157(2011) 669-74.
[3] S. Afsaneh, M. Norouz, M. Omran, A Selective and Sensitive Method for Simultaneous Determination of Traces of Paracetamol and p-Aminophenol in Pharmaceuticals Using Carbon Ionic Liquid Electrode, Electroanalysis, 20(2008) 2158-62.
[4] Z. Wang, H. Zhu, H. Zhang, G. Gao, Z. Sun, H. Liu, et al., Fabrication of the single-wall carbon nanotube compound polymer film electrode and the simultaneous electrochemical behavior of aminophenol isomers, Electrochimica Acta, 54(2009) 7531-5.
[5] M. Jamal, A.S. Sarac, E. Magner, Conductive copolymer-modified carbon fibre microelectrodes: electrode characterisation and electrochemical detection of p-aminophenol, Sensors and Actuators B: Chemical, 97(2004) 59-66.